

# Printing of Contact Holes for the 45nm Generation using Immersion Interference Lithography

Michael A. Slocum, *Student Member, IEEE*

**Abstract**— Interference lithography is a valuable tool for evaluating photoresist performance at the resolutions unattainable with conventional exposure tools. Interference lithography is most commonly used to generate one dimensional patterns such as lines and spaces. However two dimensional patterns are of much greater interest to both the resist developers and the device manufacturers in microlithography. This paper presents a technique to produce two dimensional images of contact holes at the resolution of 45nm half pitch. To our knowledge this is the highest resolution contacts printed to date using 193nm radiation. Photoresist patterns with a half-pitch of 45 nm were formed with an effective NA of 1.05 utilizing the RIT Immersion Interference system[4]. The wafer was subsequently rotated and the same pattern was printed at an angle relative to the original pattern. This double exposure technique allowed the formation of the two dimensional features. The images formed were processed, and the scanning electron micrograph (SEM) images and analysis of the data will be presented.

**Index Terms**— Contact Holes, High-NA, Immersion, Interference

## I. INTRODUCTION

As line sizes continually decrease in the microelectronic industry, more inventive ways are needed in order to characterize resists in an efficient fashion. The use of interference lithography has been refined and utilized in recent history to print very tight pitch, high NA one dimensional lines. This paper will discuss the possibilities for using the same technology to print two dimensional images.

In a conventional lithographic imaging system, the mask pattern is projected into the photoresist following being projected through a set of lenses. There are a few cases when the imaging created through interference systems and

projection systems are equivalent, and one of them occurs when a phase shift grating (1:1 duty ratio, alternating 180° phase, 100% transmission) is used with coherent illumination. The phase shift in the grating cancels the 0<sup>th</sup> diffraction order, and the  $\pm 1^{st}$  orders are captured within the entrance pupil of the system. The image that results is the interference fringes of the two plane waves that interfere at the half-angle ( $\theta$ ) created by the system.

The interference system described is only able to create a one dimensional structure which consists of lines at a constant pitch. A two dimensional image can be formed by doing one initial pass to create the one dimensional image, then using superposition to sum a second image onto the initial at an angle, preferably 90° with the first image. This will sum both passes creating an array of high and low intensity areas in a pattern much like a checkerboard.

## II. THEORY

### A. Propagation through thin film boundaries

Traditionally the numerical aperture (NA) of a system is usually defined as the sine of the half angle of the wave through air. This assumption is no longer relevant when the refractive index ( $n$ ) in Eq. 1 is no longer equal to one[2].

$$NA = n_1 \sin(\theta_1) = n_2 \sin(\theta_2) = n_3 \sin(\theta_3) \quad (1)$$

This equation is used to describe the limiting factor in an imaging system through the use of Snell's law. Since the theta value can never exceed 90° because that angle would describe total internal reflection, the NA is limited by the smallest refractive index in the system. In most current lithographic systems, the final propagation media is air, therefore the NA limit would be 1.0, but for some new state of the art systems water is used as the final media which increases the NA limit to 1.43. With this limit the maximum angle allowed in a quartz lens or prism would be 66.44° as shown in Eq. 2.

$$\theta_{qz} = \sin^{-1} \left( \frac{n_w \sin(90^\circ)}{n_{qz}} \right) = \sin^{-1} \left( \frac{1.43 \cdot 1}{1.56} \right) = 66.44^\circ \quad (2)$$

With these rules governing the way in which the information is propagated through varying media, it becomes obvious that as the refractive index of the media is increased, the possible NA of a system is increased in a directly proportional way. The NA that is defined by the propagation media can be translated into a pitch by using Eq. 3

This work is part of the senior design project requirement for a B.S. degree in Microelectronic Engineering at the Rochester Institute of Technology (RIT). The results of this project were presented at the 23<sup>rd</sup> Annual Microelectronic Engineering Conference on May 10, 2005 at RIT in Rochester, NY.

M. Slocum is with the Microelectronic Engineering department at the Rochester Institute of Technology in Rochester, NY.



$$\Lambda = k_1 \frac{\lambda_{\text{vac}}}{NA} \quad (3)$$

where  $\Lambda$  is pitch and  $k_1$  is the term that takes into account the coherency of the system. The  $k_1$  term goes to a value of 0.25 for interference systems due to the fact that the interference fringes are fully imaged. The NA used for the system in this experiment was 1.05 which results in approximately a 90nm pitch.

### B. Talbot Interference in a Prism

In order to maintain coherence in the system, a symmetric Talbot interference system was used[3], and the prism shown in Fig. 1 is described as the Smith-Talbot Prism.

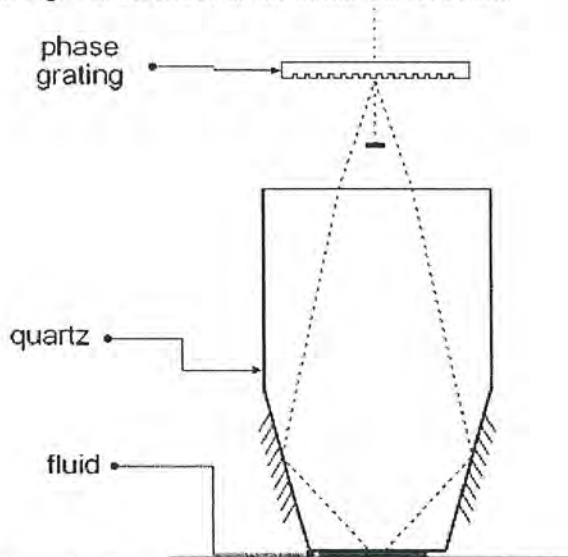


Fig. 1. Sketch of Smith-Talbot prism interference system

The phase grating acts as a beam splitter which supplies the  $\pm 1^{\text{st}}$  diffraction orders while the  $0^{\text{th}}$  order is blocked. (if any exists due to the mask gratings not being exactly  $180^\circ$  out of phase) The turning mirror is created by depositing a reflective coating onto the facets of the quartz prism. The angle of the facets as well as the pitch of the phase gratings defines the angle of the interference beams as they enter the resist. The top surface of the prism has a quarter wave anti-reflective coating in order to minimize any stray light. The bottom of the prism along with the wafer surface forms a fluid gap which can be used to trap the water used in this immersion system.

This system is designed to be used with a beam that has a small spatial and temporal coherence lengths. The spatial coherence is needed in order to ensure that the interfering waves do not come from different parts of the incoming beam which will cause a reduction in the fringe visibility. The temporal coherence of the incoming beam is desired to be within the optical path difference (OPD) created by the varying lengths that the diverging beams must travel when they do not converge at the very center of the prism. Both of the temporal and spatial coherence needs form the requirement that the resultant image must be formed at the center of the prism in order to achieve the desired fringes.

### C. Interference System

In order to fulfill the coherence requirements of the system, the laser has to meet many requirements. The laser used for the system is a Lambda Physik 193nm line narrowed laser. The system is depicted in Fig. 2.

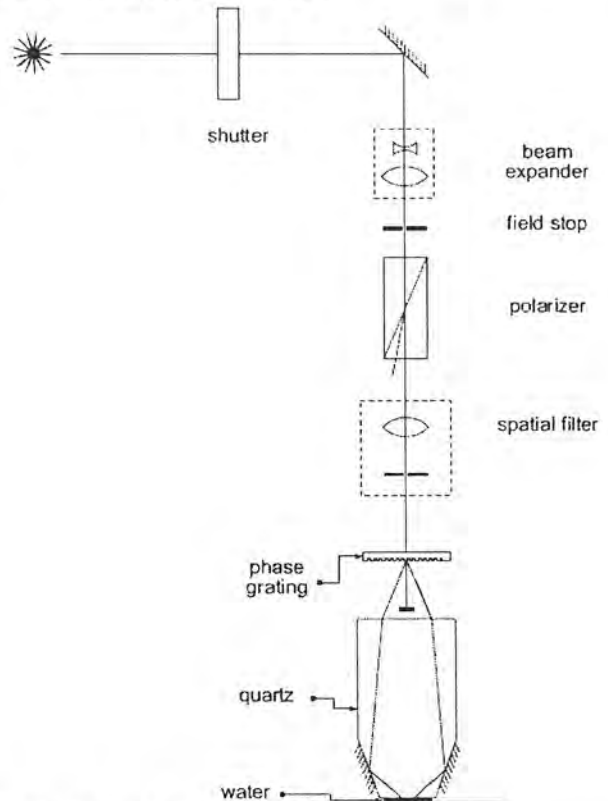


Fig. 2. Sketch of Smith-Talbot prism interference system

The 5x beam expander is used to increase the usable beam size from 0.5mm to 2.5mm. The 2.5mm field is then defined by the field stop in order to limit the field to a size that maintains the spatial and temporal coherence required for the system. Polarization is maintained by the Rochon prism  $\text{MgF}_2$  polarizer which can restrict the beam to solely TM, TE or any value of partial polarization. In order to improve the uniformity of the beam and filter out the high frequency information a spatial filter is needed. The spatial filtering consists of a lens which focuses the beam into a  $50\mu\text{m}$  pinhole that completes the filtering process. The beam splitting phase grating mask was designed with a pitch of 600nm to create the desired angle of the diverging beams. For this experiment the Smith Talbot prism with an effective NA of 1.05 was used which results in lines having a pitch of 90nm.

### D. Double pass image summation

Since traditional interferometric imaging is restricted to a single dimension as it is described in Eq. 4, and depicted in Fig. 3, a new method of forming the image must be designed in order to create a two dimensional image in the resist. The equation which describes the interference system takes into account the beams field intensity  $|E_{01}|$  which is equivalent in both directions, the propagation vector  $k$ , the oblique



intersection angle, and the position of intersection on the x-axis.

$$I \propto 2|\bar{E}_{o1}|^2 [1 + \cos(2kx \sin \theta)] = 4|\bar{E}_{o1}|^2 \cos^2(kx \sin \theta) \quad (4)$$

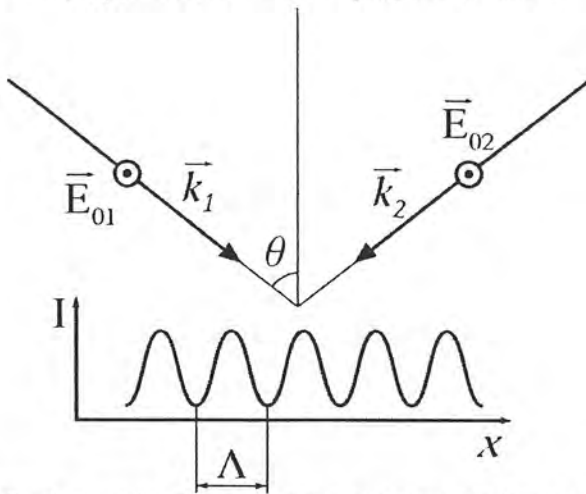


Fig. 3. Depiction of incoming waves which form interference fringes with pitch dependent upon the incoming oblique angle

As a result of this equation, the only way two-dimensional objects can be formed is by using superposition to sum two one-dimensional arrays into one two-dimensional array. This can be done by summing the aerial images in Fig. 4, and Fig. 5 to create the new image seen in Fig. 6 and 7.

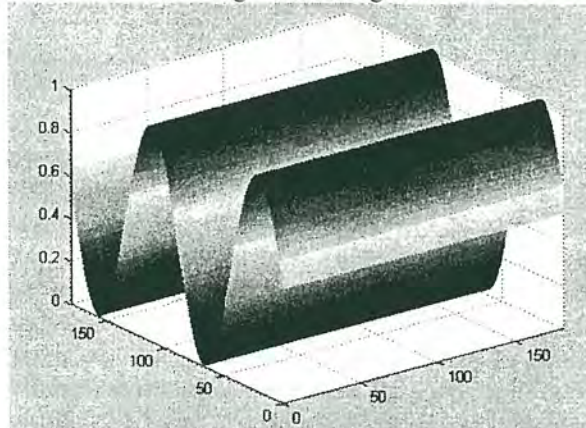


Fig. 4. One-dimensional aerial image created by first pass in x direction

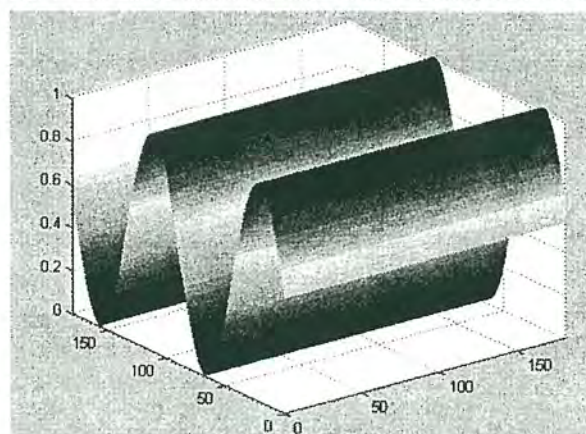


Fig. 4. One-dimensional aerial image created by first pass in x direction

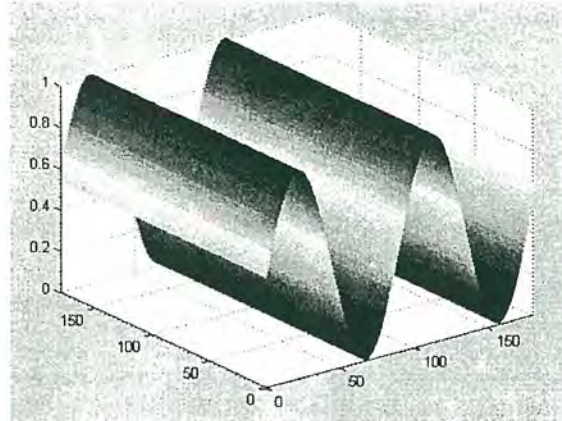


Fig. 5. One-dimensional aerial image created by second pass in y direction

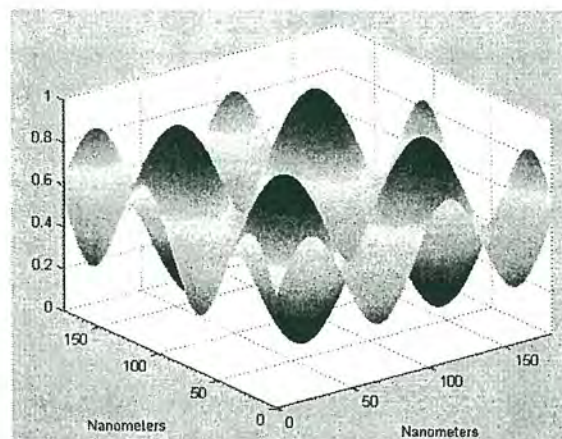


Fig. 6. Two-dimensional aerial image created by summation of x and y directional passes depicted in 3-d

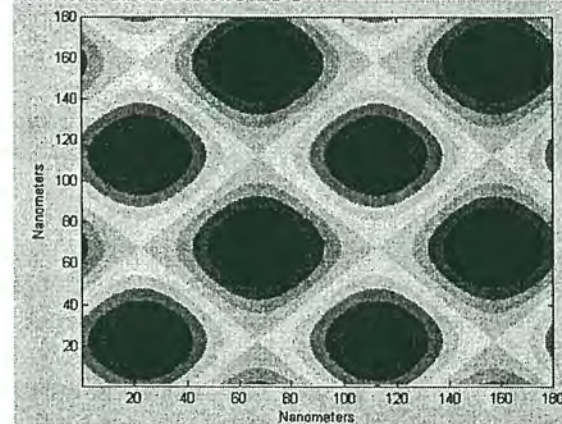


Fig. 7. Two-dimensional aerial image created by summation of x and y directional passes shown in a top-down view

Given the fact that a second pass is needed to create the two-dimensional images, the passes do not have to be in orthogonal directions. There are a few motivations for imaging the second pass in an angle other than 90° which consist of additional degrees of freedom, the fact that varying the angle alters the pitch in the diagonal directions. The varying pitch can provide further analysis of resist performance which can be very important for characterizing resists. A top down image of two passes that are formed when the images are summed at 60° apart is shown in Fig. 8.



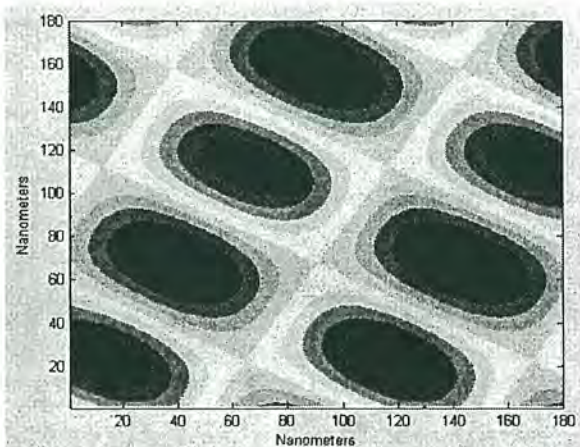


Fig. 8. Two-dimensional aerial image created by summation of x directional and 60° pass shown in a top-down view

### III. EXPERIMENTAL

The way in which the two-dimensional images are formed in orthogonal directions without the use of an automated alignment system had to be designed for the experiment to proceed. The alignment procedure was designed to use the orthogonal faces of the prism along with the edges of a cleaved wafer. The wafer piece was aligned to two faces of the prism, then the piece was rotated 90° and the same sides of the wafer were then aligned to two faces on the prism. The alignment procedure is depicted in Fig. 9.

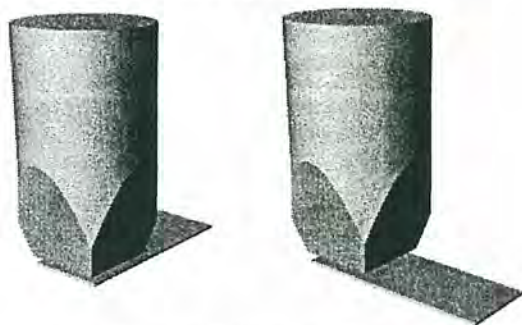


Fig. 9. Alignment system for forming 2-d structures by using the edges of the prism and cleaved edge of wafer

The film stack also had to be optimized in order to obtain an image with such a high NA since these processing conditions result in a devastating high amount of standing waves if the stack is not optimized. The resist thickness becomes very easy to optimize, since the main concern for these images becomes the aspect ratio since resists at 45nm half pitch cannot maintain an aspect ratio greater than 2:1. With this limitation taken into account the resist thickness was chosen to be 80nm, and the spin speed was calculated to achieve that thickness. Following the choice of a resist thickness, the BARC (bottom anti-reflective coating) thickness had to be chosen to reduce the reflection from the BARC which will in turn reduce the standing waves in the resist. The BARC thickness was optimized by using a program, ILSim[1] shown in Fig. 10.

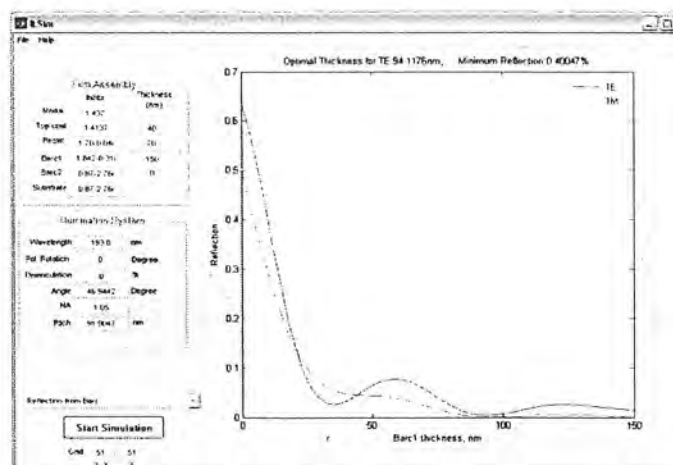


Fig. 10. Screenshot of ILSim - Reflectivity simulation program to optimize the BARC thickness to reduce reflectivity from the BARC surface

The program evaluates the reflection from surfaces in the film stack for a particular propagation angle from the refractive index term for resist and BARC that is input into the program. The inputs for the program are the real and imaginary terms of the refractive index ( $n$  &  $k$ ) for the resist (TOK ILP-12) and the BARC (Brewer Science AR29A-8). The program returns the reflection normalized to the incoming intensity for varying thicknesses for the BARC layer. From the program a BARC thickness of 94.1176nm results in reflection from the film layer of 0.40047% which is very low and results in a minimal amount of standing waves in the resist film.

### IV. RESULTS

The Talbot interference system with an effective NA of 1.05 was used initially in a single pass capacity in order to get the dose to size ( $E_s$ ) for the stack. The  $E_s$  term is used to quantify the thresholding of the exposure which is used to determine whether the resulting image will be a contact hole or a resist post. With the stack that was used for this experiment the  $E_s$  was found to be 16mJ/cm<sup>2</sup>, which is actually an undesirably fast dose for the experiment. The smaller  $E_s$  is due to the resist being a fast acting line resist instead of a contact hole resist which traditionally has a much higher  $E_s$ . The need for a higher dose to size for the 2-d printing is due to the fact that a very high precision in dose is needed across the entire wafer in order to create equal pitch lines, and this can be done more easily by having a slower acting resist. The first results were produced using a threshold of  $0.44 \cdot E_s$  for both passes in order to create contact holes in the positive photoresist that was used for these exposures. The SEM image of the contact hole structures is shown in Fig. 11, and the simulation results using the resist threshold model is shown in Fig. 12.



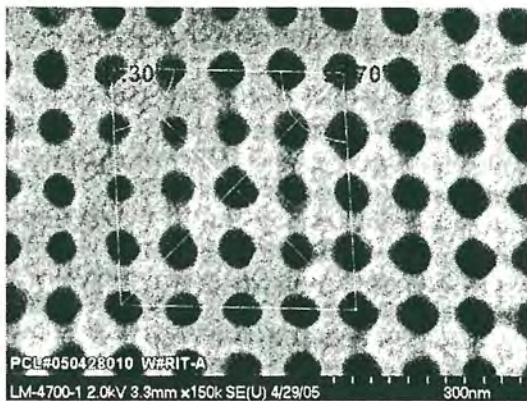


Fig. 11. SEM image of contact hole structures imaged with  $0.44 \cdot E_s$  in both directions

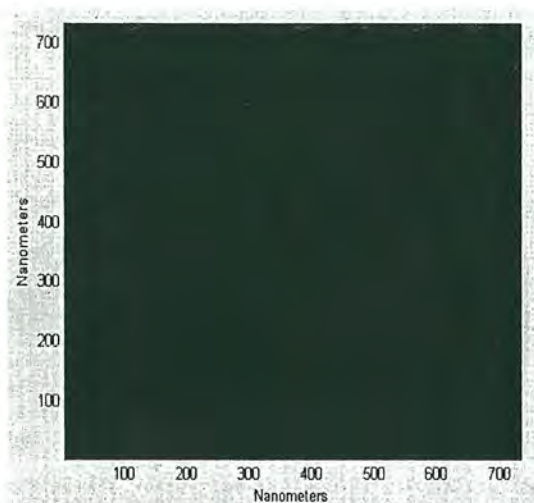


Fig. 12. Simulation of resist post structures with resist threshold model

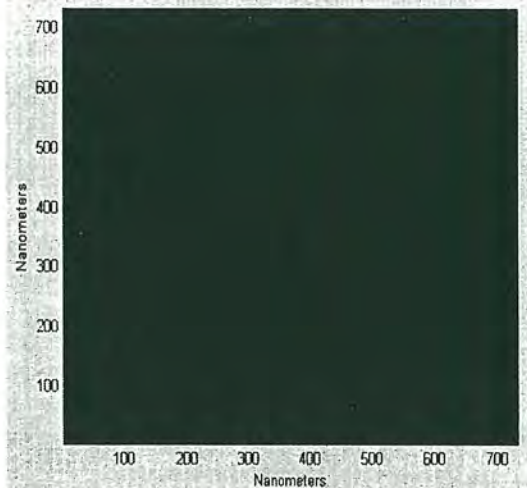


Fig. 12. Simulation of contact hole structures with resist threshold model

Additional exposures in the experiment were designed to form resist posts by thresholding the exposure at a higher value of  $0.56 \cdot E_s$  or a  $9 \text{ mJ/cm}^2$  exposure. The SEM image of the resist post structures is shown in Fig. 13, and the simulation result using the resist threshold model is shown in Fig. 14.

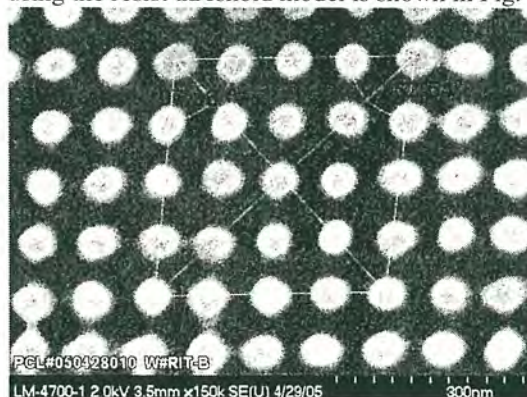


Fig. 11. SEM image of resist post structures imaged with  $0.56 \cdot E_s$  in both directions

## V. CONCLUSION

The double pass exposure system was used with the interferometric immersion system in order to create contact holes and resist poles on a  $90 \text{ nm}$  pitch grid. The use of thresholding the exposures at varying values was used to change the resultant image from contact holes to resist posts depending on the threshold chosen. It was found that a threshold of  $0.44 E_s$  is optimal for contact holes while  $0.56 E_s$  is the best dose to create resist posts.

Double pass exposures with interferometric lithography has proved to be a simple way to achieve a very tight pitch grid without having to deal with the many concerns and costs of creating these images with a traditional projection system. As a result of the ease in creating these very small pitch grids this method becomes extremely useful in characterizing contact hole resists for the future process nodes. This method can be used to print contact holes that are only limited in pitch by the refractive index of the materials being used to propagate the beam. Historically the restrictive media has been the medium between the lens and the resist stack, but with the possibility of high refractive index propagation media the restriction can easily become the resist.

## VI. REFERENCES

- [1] Y. Fan, A. Bourov, L. Zavyalova, J. Zhou, A. Estroff, N. Lafferty, B.W. Smith, "ILSim - A compact simulation tool for interferometric lithography", *Proc SPIE* 5754, (2005)
- [2] B.W. Smith, A. Bourov, Y. Fan, L. Zavyalova, N. Lafferty, F. Cropanese, "Approaching the numerical aperture of water - immersion lithography at  $193 \text{ nm}$ ", *Proc. SPIE* 5377, (2004)
- [3] A. Bourov, Y. Fan, F. Cropanese, N. Lafferty, L. Zavyalova, H. Kang, B.W. Smith, "Immersion microlithography at  $193 \text{ nm}$  with a Talbot prism interferometer", *Proc. SPIE* 5377, (2004)

- [4] B.W. Smith, H. Kang, A. Bourov, F. Cropanese, Y. Fan, "Water immersion optical lithography for the 45nm node", *Proc. SPIE* 5040, (2003)

## VII. ACKNOWLEDGMENTS

The author acknowledges the following: Anatoly Bourov for his excellent assistance in creating images used for the report, Yongfa Fan for his help creating the simulation program used to model the double pass and assistance with the exposure system, Emil Piscani for his help designing the alignment procedure for the exposures, Dr. Bruce Smith for his guidance and assistance as project advisor, SEMATECH for the donation of wafers and high resolution SEM images as well as support for the tool used in creating the images and Photonics for the donation of the mask used in the interferometric system.